DOI: http://dx.doi.org/10.22104/ijhfc.2016.486

Iranian Journal of Hydrogen & Fuel Cell 4(2016) 301-313

Iranian Journal of Hydrogen & Fuel Cell

IJHFC

Journal homepage://ijhfc.irost.ir

Effect of recycling solid oxide fuel cell products on the performance of a SOFC-Gas turbine hybrid system

M. Rajabinasab[1], Mehran Ameri[2*], M. Iranmanesh[1], S. Sadeghi[3]

[1]Institute of Energy, Graduate University of Advanced Technology, Kerman, Iran
[2]Department of Mechanical Engineering, Shahid Bahonar University, Kerman, Iran
[3]Department of Mechanical Engineering, Graduate University of Advanced Technology, Kerman, Iran

Article Information

Article History:

Received:
06 Feb 2017
Received in revised form:
27 Mar 2017
Accepted:
29 Apr 2017

Keywords

Hybrid system
Solid oxide fuel cell
Gas turbine
Cathode product recycling
Anode product recycling

Abstract

In this study, the effect of recycling fuel cell products on the performance of a solid oxide fuel cell and gas turbine (SOFC-GT) hybrid system was investigated. Three types of products recycling are considered: cathode products recycling (CPR), anode products recycling (APR), and both cathode and anode products recycling (BACPR). In the present work, operating temperature and limiting current density was calculated from governing equations by the trial and error method. Furthermore, the effect of pressure ratio and air utilization factor on the performance of the SOFC-GT hybrid system is considered. Results show that CPR has more effect on the performance of hybrid systems than APR. The total electrical efficiency of the hybrid system increases as the cathode recycle ratio (CRR) increases and decreases as the anode recycle ratio (ARR) decreases. In addition, results show that the hybrid system with BACPR can achieve a higher overall electrical efficiency of approximately 75%.

1. Introduction

A fuel cell is a device that generates electricity by a chemical reaction. The energy of a fuel gas changes directly into electrical energy without the need for direct combustion. Fuel cells are generally classified by the operation temperature. Among the different types, solid oxide fuel cell (SOFC) technology is very promising because of its high efficiency, little pollution, noiselessness, absence of moving parts, fuel flexibility, and high temperature of the exhaust heat, which can be used for cogeneration or bottoming cycles for additional electricity generation [1].

Among all types of fuel cells, the solid oxide fuel

*Corresponding Author's Fax: +98 3412120964
E-mail address: ameri_mm@uk.ac.ir

cell can operate at high temperatures (between 600 to 1000°C) [2]. Because of the high operating temperature of solid oxide fuel cells, they are capable of internally reforming fuel gases without the use of a reforming catalyst [2]. In addition, the high operating temperature creates the capacity for increasing efficiency. Further improvement in efficiency can be achieved by combining a SOFC with common heat engines like gas turbines. Results have shown that efficiency can reach 70% by combining a SOFC and gas turbine (GT) [3]. Therefore, SOFC-GT hybrid systems have attracted the attention of many researchers worldwide because of the increase in efficiency, ability of heat recycling, and producing electrical power in various capacities. Chan et al. [4] presented a full analysis of the overpotential in the tubular solid oxide fuel cell. They used the Butler Volmer equation rather than simplified expressions, such as the Tafel equation and linear current potential equation, for analyzing the activation overpotential. In addition, they used the ordinary diffusion factor and Knudsen diffusion factor for analyzing the concentration overpotential. In these studies, the effect of the thickness of different components of a solid oxide fuel cell on the overpotential of cells was shown. Chan et al. [5] worked on modeling a SOFC-GT hybrid system fed by natural gas. They investigated the effect of parameters, such as operating pressure and fuel flow rate, on the performance of each component and total hybrid system. Volkan et al. [6] presented the effects of operating temperature and operating pressure on the performance of a solid oxide fuel cell. Ghanbari Bavarsad et al. [7] analyzed the SOFC-GT hybrid system based on the first and second law efficiency of thermodynamics. They carried out a parametric study in order to investigate the effect of parameters such as the fuel flow rate, air flow rate, operating temperature, and operating pressure. Pirkandi et al. [8] introduced the SOFC-GT hybrid system as a power and heat cogeneration system. They examined the effect of different parameters such as operating temperature and operating pressure of a fuel cell, fuel utilization factor, and ratio of air to fuel on the performance of the hybrid system. They achieved a 73% total efficiency (heat and electrical efficiency) by considering the optimum ratio of air to fuel and the optimum fuel utilization factor.

In recent years, much research has been done on the types of configuration and the effect of different parameters on the performance of SOFC-GT hybrid systems, but less attention has been paid to the effect of fuel cell products' recycling. In this study, three configurations of hybrid systems used to recyle SOFC products are considered. These configurations consist of a hybrid system with CPR, a hybrid system with APR, and a hybrid system with BCAPR. These types of configurations are also compared with a standard hybrid system in similar conditions.

2.Description of the standard SOFC-GT hybrid system

A schematic diagram of the plant layout of a standard SOFC-GT hybrid system is shown in Fig. 1. This system consists of a compressor, solid oxide full cell, combustion chamber, gas turbine, mixer, heat exchanger, and pump. Air enters the compressor in environmental condition (spot1) and exits in a compressed state (spot2). Compressed air (spot2) enters the heat exchanger and its temperature increases by recovering the heat of the gas turbine's exhaust gases. The exited compressed hot air from the heat exchanger (spot3) enters the cathode of fuel cell. On the other path, the fuel

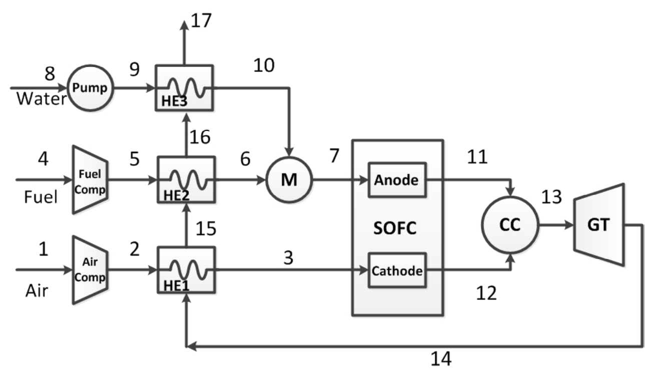

Fig. 1. Schematic of standard SOFC-GT hybrid system

passes through the compressor (spot4) and heat exchanger (spot5) and then enters the mixer with high pressure and high temperature. The required steam for internal reforming and shifting reactions in the fuel cell is supplied independently. For this purpose, water enters the pump in environmental conditions (spot8). The pumped water (spot9) enters the heat exchanger and evaporates by the heat recovery of the gas turbine's exhaust gases (spot10). The steam and fuel are combined in the mixer and enter the anode of the fuel cell (spot7). Both the anode and cathode products (spot11 and 12) enter the combustion chamber and then the produced hot gases enter the gas turbine to generate electrical power (spot13). For heat recovery, the turbine exhaust gases (spot14) will pass through three heat exchangers to warm up air, fuel, and water (spots 15, 16 and 17).

3.Hybrid System modeling

The following general assumptions and conditions are considered for modeling the hybrid system:

-All components of the hybrid system are considered as a control volume.

- All gases in the hybrid system are considered as ideal gas.
- The fluid flow in all components is considered steady state with negligible frictional losses.
- There is no gas leak from the hybrid system.
- Uniform temperature and pressure distribution is assumed in all components of the hybrid system.
- The chemical reactions are considered steady state.
- Change of potential and kinetic energies are considered negligible in all processes.
- Temperature of the anode and cathode outlet is assumed to be equal to the operating temperature of the solid oxide fuel cell.

The governing equations for modeling the components of the hybrid system are presented in this section. Each component is modeled separately by solving simultaneous mass and energy balance equations. First, the solid oxide fuel cell is modeled in three separate parts: internal reforming, thermal, and electrochemical.

3.1. Solid oxide fuel cell

The fuel cell used in this study is a type of tubular solid oxide fuel cell with internal reforming. For a fuel cell fed by a conventional fuel like natural gas, reforming is needed to convert the fuel into hydrogen. In the reforming process, steam is required; it is obtained by the evaporation of feed water by the recovered heat of the gas turbine exhaust gases.

As reforming is done inside the cell, it is assumed that the mechanism of reactions taking place inside the cell is as follows [5]:

Steam reforming $x \rightarrow [CH_4 + H_2O \rightarrow CO + 3H_2]$ (1)

Water gas Shifting $y \rightarrow [CO + H_2O \rightarrow CO_2 + H_2]$ (2)

Electrochemical reaction $z \rightarrow [H_2 + \frac{1}{2}O_2 \rightarrow H_2O]$ (3)

The hydrogen produced by reforming and shifting reactions with the available oxygen in the air participates in the electrochemical reaction. Although some of the carbon monoxide also participates in the electrochemical reaction, the main reaction is related to hydrogen [9]. In the above relations, x, y, and z are the molar rates of reaction progress for steam reforming, water-gas shifting, and electrochemical reactions, respectively.

As the reforming and shifting reactions are in equilibrium state, the equilibrium constants of the reactions can be calculated according to equations 4 - 7 [5].

$$Kp_r = \frac{P_{H_2}^3 \times P_{CO}}{P_{CH_4} \times P_{H_2O}} \quad (4)$$

$$Kp_{sh} = \frac{P_{CO2} \times P_{H_2}}{P_{CO} \times P_{H_2O}} \quad (5)$$

$$Kp_r = \frac{([\dot{n}_{H_2}]_{in} + 3x + y - z)^3 \times ([\dot{n}_{CO}]_{in} + x - y)}{([\dot{n}_{CH_4}]_{in} - x) \times ([\dot{n}_{H_2O}]_{in} - x - y + z)} \times \frac{P_{cell}^2}{([\dot{n}_{tot}]_{in} + 2x)^2} \quad (6)$$

$$Kp_{sh}=\frac{([\dot{n}_{CO_2}]_{in}+y)\times([\dot{n}_{H_2}]_{in}+3x+y-z)}{([\dot{n}_{CO}]_{in}+x-y)\times([\dot{n}_{H_2O}]_{in}-x-y+z)} \quad (7)$$

The equilibrium constants of reforming and shifting reactions are directly correlated to the temperature by a polynomial equation [5]:

$$LogKp=AT^4+BT^3+CT^2+DT+E \quad (8)$$

where, A, B, C, D, and E are experimental constants whose values have been listed by Chan [5]. The fuel utilization factor (U_f) in the anode side is defined as the ratio of reacted hydrogen to the produced hydrogen [8].

$$U_F=\frac{z}{4\dot{n}_{CH_{4,in}}+\dot{n}_{H_{2,in}}+\dot{n}_{CO_{in}}} \quad (9)$$

The reversible voltage of fuel cell is calculated by Nernst equation [2]:

$$E=E^0+\frac{R_uT}{n_eF}\ln(\frac{P_{H_2}\times P_{O_2}^{\frac{1}{2}}}{P_{H_2O}}) \quad (10)$$

Where E^0 is the voltage of the fuel cell in standard conditions, R_u is the universal gas constant, T is the operating temperature of the fuel cell, F is the Faraday's constant, and n_e is the number of circulated electron in circuit for the formation of each water molecule. The real voltage of the fuel cell is less than the Nernst voltage due to irreversibility in the fuel cell. This irreversibility can be divided into three groups: activation loss, ohmic loss, and concentration loss. The value of real voltage is calculated according to equation (11) [2]:

$$V_{cell}=E-(V_{act}+V_{ohm}+V_{conc})=E-\Delta V_{loss} \quad (11)$$

The value of activation losses is equal to the sum of activation losses of the anode and cathode, and will be obtained by simplifying the Butlere-Volmers equation [6]:

$$V_{act}=V_{act_{an}}+V_{act_{ca}} \quad (12)$$

$$V_{act}=\frac{2R_uT}{n_eF}Sinh^{-1}(\frac{i}{2i_0}) \quad (13)$$

where i and i_0 are the current density and the exchange current density, respectively.

The ohmic losses are related to the transfer of electrons and ions in the anode, cathode, electrode, and internal connectors. The ohmic losses are obtained by equations 14-17 [6]:

$$V_{ohm}=V_{ohm_{an}}+V_{ohm_{ca}}+V_{ohm_{el}}+V_{ohm_{int}} \quad (14)$$

$$V_{ohm}=ir \quad (15)$$

$$r=\delta\rho \quad (16)$$

$$\rho=Aexp(\frac{B}{T}) \quad (17)$$

The values of A, B, and δ in equations (16) and (17) are constant parameters that depend on the geometry and type of the fuel cell. The values of these parameters have been listed by V. Akkaya [6].

The value of concentration losses is calculated by the following equations [6]:

$$V_{conc}=V_{conc_{an}}+V_{conc_{ca}} \quad (18)$$

$$V_{conc_{an}}=\frac{R_uT}{n_eF}\ln(\frac{1-\frac{i}{i_{L,H_2}}}{1+\frac{i}{i_{L,H_2O}}}) \quad (19)$$

$$V_{conc_{ca}}=\frac{R_uT}{n_eF}\ln(\frac{1}{1-\frac{i}{i_{L,O_2}}}) \quad (20)$$

where, iL is the limiting current density.

The power generated by a SOFC can be calculated based on the real voltage of the fuel cell by equations (21) to (23):

$$I_{tot}=2Fz \quad (21)$$

$$\dot{W}_{sofc_{DC\_tot}}=V_{cell}\times I_{tot} \quad (22)$$

$$\dot{W}_{sofc_{AC\_tot}}=\dot{W}_{sofc_{DC\_tot}}\times\eta_{invt,sofc} \quad (23)$$

where I_{tot} is the total current of the fuel cell and $\eta_{invt,sofc}$ is the coefficient of inversion of direct to alternative current in the fuel cell.

Since the reforming reaction is endothermic and the shifting reaction is exothermic, the value of heat produced from the reforming and shifting reactions are obtained by [5]:

$$\dot{Q}_r = x(\overline{h}_{CO} + 3\overline{h}_{H_2} - \overline{h}_{CH_4} - \overline{h}_{H_2O}) \tag{24}$$

$$\dot{Q}_{sh} = y(\overline{h}_{CO_2} + \overline{h}_{H_2} - \overline{h}_{CO} - \overline{h}_{H_2O}) \tag{25}$$

The heat produced from electrochemical reaction is supplied from two main sources. One is due to the irreversibility reaction and the other due to the voltage losses of the fuel cell. The value of the heat produced from the electrochemical reaction also is calculated as follows [5]:

$$\dot{Q}_{elec} = zT\Delta S - I_{cell}\Delta V_{Loss} \tag{26}$$

$$\Delta S = (S^0_{H_2O} - S^0_{H_2} - \frac{1}{2}S^0_{O_2}) + \frac{R_u}{2}\ln(\frac{P^2_{H_2} \times P_{O_2}}{P^2_{H_2O}}) \tag{27}$$

The total net heat transfer of the solid oxide fuel cell is obtained by calculating the difference between the heat values of the three above reactions and the following equation:

$$Q_{net} = \dot{Q}_{elect} + \dot{Q}_{sh} - \dot{Q}_r \tag{28}$$

The temperature of outflow gasses from the fuel cell can be calculated by balancing the energy, and also through the use of the trial and error method. The first law of thermodynamics for the fuel cell is as follows [8]:

$$(\dot{n}_{i_{ca_{in}}}\overline{h}_{i_{ca_{in}}} + \dot{n}_{i_{an_{in}}}\overline{h}_{i_{an_{in}}}) = \dot{Q}_{surr} + \dot{W}_{sofc_{DC\_tot}} + (\dot{n}_{i_{ca_{out}}}\overline{h}_{i_{ca_{out}}} + \dot{n}_{i_{an_{out}}}\overline{h}_{i_{an_{out}}}) \tag{29}$$

3.2. Compressor

Assuming an adiabatic compression process and applying Eqs. 30-32 for the system, one may find the temperature of outlet gases, pressure ratio, isentropic efficiency and the work required for the compressor [10]:

$$\frac{T_{out_{is}}}{T_{in}} = (\frac{P_{out}}{P_{in}})^{\frac{k_a-1}{k_a}} = (PR_{comp})^{\frac{k_a-1}{k_a}} \tag{30}$$

$$\eta_{comp} = \frac{W_{comp_{is}}}{W_{comp}} = \frac{\overline{h}_{out_{is}} - \overline{h}_{in}}{\overline{h}_{out} - \overline{h}_{in}} = \frac{T_{out_{is}} - T_{in}}{T_{out} - T_{in}} \tag{31}$$

$$\dot{W}_{comp} = \dot{n}_a(\overline{h}_{out} - \overline{h}_{in}) \tag{32}$$

3.3. Gas turbine

By knowing the turbine inlet temperature and the definition of isentropic efficiency of the gas turbine, the value of actual work and exhaust gas temperature can be calculated according to [10]:

$$\frac{T_{in}}{T_{out_{is}}} = (\frac{P_{in}}{P_{out}})^{\frac{k_g-1}{k_g}} = (PR_{gt})^{\frac{k_g-1}{k_g}} \tag{33}$$

$$\eta_{gt} = \frac{W_{gt}}{W_{gt_{is}}} = \frac{\overline{h}_{in} - \overline{h}_{out}}{\overline{h}_{in} - \overline{h}_{out_{is}}} = \frac{T_{in} - T_{out}}{T_{in} - T_{out_{is}}} \tag{34}$$

$$\dot{W}_{gt} = \dot{n}_g(\overline{h}_{in} - \overline{h}_{out}) \tag{35}$$

3.4. Combustion chamber

Because only a portion of inlet fuel and air are consumed in the fuel cell, the role of a combustion chamber is to increase the system efficiency and reduce the pollution. The outlet gases of the fuel cell, which consist of steam, carbon dioxide, carbon monoxide, hydrogen, and methane in the anode side and oxygen and nitrogen in the cathode side, are reacted in the combustion chamber [8]:

$$CH_4 + 2O_2 \rightarrow CO_2 + 2H_2O \tag{36}$$

$$CO + \frac{1}{2}O_2 \rightarrow CO_2 \tag{37}$$

$$H_2 + \frac{1}{2}O_2 \rightarrow H_2O \tag{38}$$

All of the above reactions are exothermic and cause the temperature rise of outlet gases of the combustion chamber. The temperature of outlet gases of the combustion chamber can be calculated by the energy conservation equation and considering the efficiency of the combustion chamber as follows [8]:

$$\dot{n}_{i_{ca_{out}}} \bar{h}_{i_{ca_{out}}} + \dot{n}_{i_{an_{out}}} \bar{h}_{i_{an_{out}}} - \dot{n}_{i_{cc_{out}}} \bar{h}_{i_{cc_{out}}} + \dot{Q}_{loss_{cc}} = 0 \tag{39}$$

where is the heat losses of the combustion chamber, its value depends on the efficiency of the combustion chamber and fuel heat value (LHV). The heat losses caused by combustion reaction are calculated by:

$$\dot{Q}_{loss_{cc}} = \dot{Q}_{loss_{ccCH_4}} + \dot{Q}_{loss_{ccCO}} + \dot{Q}_{loss_{ccH2}} \tag{40}$$

$$\dot{Q}_{loss_{ccCH_4}} = \dot{n}_{CH_{4ca_{out}}} (1-\eta_{cc}) \times \mathrm{LHV}_{CH_4} \tag{41}$$

3.5. Heat exchanger

In this study, three external heat exchangers fed by the hot exhaust gases of the gas turbine are used to provide the required steam to increase the temperature of the inlet air and fuel and provide the required steam. ,are used, which are. The temperature of outlet gases from the heat exchanger is calculated based on the effectiveness-number of transfer unit method (ε_{HE} –NTU) [11]:

$$\varepsilon_{HE} = \frac{C_c(\mathrm{T}_{C_{out}} - \mathrm{T}_{C_{in}})}{C_{\min}(\mathrm{T}_{h_{in}} - \mathrm{T}_{C_{in}})} = \frac{C_h(\mathrm{T}_{h_{in}} - \mathrm{T}_{h_{out}})}{C_{\min}(\mathrm{T}_{h_{in}} - \mathrm{T}_{C_{in}})} \tag{42}$$

$$m_c\, \mathrm{c}_c(\mathrm{T}_{C_{out}} - \mathrm{T}_{C_{in}}) = m_h\, \mathrm{c}_h(\mathrm{T}_{h_{in}} - \mathrm{T}_{h_{out}}) \tag{43}$$

3.6 Pump

The required work for the pump can be obtained by [8]:

$$\dot{W}_{pump} = \dot{n}_{water} v_{water_{in}} (\mathrm{P}_{out} - \mathrm{P}_{in}) \tag{44}$$

3.7. Mixer

The temperature of the mixer outlet can be obtained by:

$$\dot{n}_{in} \bar{h}_{in} - \dot{n}_{out} \bar{h}_{out} + \dot{Q}_{loss_{Mix}} = 0 \tag{45}$$

3.8. Hybrid system

Considering the total hybrid system as a control volume, the electrical efficiency and net output power are obtained by the following equations [8]:

$$\eta_{elect_{NET}} = \frac{\dot{W}_{NET}}{\dot{n}_{fuel} \times LHV} \tag{46}$$

$$\dot{W}_{NET} = \dot{W}_{sofc} + \dot{W}_{gt} - \dot{W}_{comp_a} - \dot{W}_{comp_f} - \dot{W}_{pump} \tag{47}$$

4. Results

For plant simulation, the governing equations are solved by EES software. Change in the thermodynamic properties of the hybrid system is calculated. The hybrid system consists of an internal reformer, SOFC stack, combustion chamber, gas turbine, air and fuel compressors, pump, mixers, and heat exchangers. The operating temperature of the fuel cell is one of the important parameters in analyzing the performance of the hybrid system. First, the program guesses an operating temperature for the fuel cell. Then, the reforming, electrochemical, and thermal nonlinear equations are solved simultaneously using the guessed operating temperature and the new operating temperature of the fuel cell was obtained. Then all equations related to other components of the hybrid system are solved. This process continues until the convergence condition is established. To validate this model the computed results for the attained polarization curve are compared with the published experimental results by Singhal [3]. As it is seen in Fig. 2., they are almost compatible. Unfortunately, experimental performance data for the fuel cell is not readily available for methane or natural gas. Moreover, the obtained results of the general hybrid system are compared with the model from Calise et al. [12]. The proximity of the results, tabulated in Table 1, show the suitability of this model.

The purpose of this study is to investigate the effect

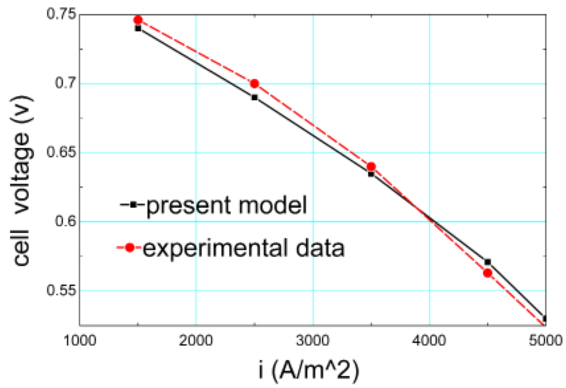

Fig. 2. Comparison of experimental data[3] and present model results for cell voltage.

Table 1. The Comparison of present model results and Calise et al [15]

Parameter	Present study	Calise et al [15]	Error (%)
Operating temperature of SOFC	1033	1020	1.27
temperature of input compound into GT	1157	1150	0.6
power output from SOFC	1208	1220	0.98
power output from GT	360.4	342	5.3
SOFC electrical efficiency	0.527	0.532	0.94
system electrical efficiency	0.6845	0.6815	0.44

of parameters such as the recycle rate of fuel cell products, the air utilization factor, and the pressure ratio on the performance of the hybrid system. The input parameters are depicted in Table 2 for the simulation of the hybrid system.

The standard hybrid system (S-HS) is a sample of a general SOFC-GT hybrid system that has been studied by numerous researchers. In this model, no recycled fuel cell products are used, and the required steam for reforming and shifting reactions is provided by the evaporation of water. A schematic of a standard hybrid system is shown in Fig. 1. The results of the simulation of the hybrid system are shown in Table 3.

In the second type of the hybrid system, the cathode products of the fuel cell are recycled (Fig. 3). These products consist of oxygen and nitrogen and are mixed with the inlet air. Therefore, the flow rate of inlet air to the hybrid system and so the power consumed by the air compressor is reduced In CPR, the temperature of the cathode inlet increases and so the operating temperature, power output and efficiency of the fuel cell increase. In CPR-HS, it is important to mention that the amount of CPR must be selected carefully so that the combustion chamber contains enough oxygen to reach the complete combustion of methane, hydrogen, and carbon monoxide. To compare the S-HS and the CPR-HS, the value of anode products entering the combustion chamber is equal, but the amount of oxygen and nitrogen entering the combustion chamber of the CPR-HS decreases. Consequently, for the same amount of input fuel into the combustion chamber, the amount of combustion chamber outlet gases decreases for CPR-HS. Therefore, the temperature of the output products from the combustion chamber and input gases into the gas turbine for CPR-HS is more than that for the S-HS. Overall, the net power output for CPR-HS is more than that for S-HS. The results of the simulation of CPR-HS are shown in Table 4. When CRR increases, the fuel cell operating temperature and the temperature of gas turbine inlet will increase. It should also be noted that the amount of CRR must be limited to a specific value to avoid an excessive increase of operating temperature, which can lead to

Table 2. Input parameters for SOFC-GT hybrid system.

Value	Parameter	Value	Parameter
$\dot{n}_{fuel}(Kmol/s)$	0.003	$\eta_{is\_comp\_air}$	0.81
U_F	0.85	$\eta_{is\_comp\_fuel}$	0.81
U_a	0.25	η_{is_GT}	0.85
$A_{cell}(m^2)$	0.1036	η_{is_pump}	0.8
$i(A/m^2)$	3000	$\eta_{inverter}$	0.98
$T_0(K)$	298	η_{cc}	0.98
$P_0(bar)$	1	ε_{HE}	0.9
LHV_{CH_4}(Kj/ mol)	802.3	r_{sc}	2
PR	3	ΔP_i	0.02

Table 3. Results of simulation of the S-HS.

Parameter	Value
Input air flow rate (kmol/s)	0.09714
Power consumed by the air compressor (kw)	382.4
Power output of GT (kw)	930.4
Power output of SOFC (kw)	1091
Net power output of system (kw)	1627
Operating temperature of SOFC (°C)	1143
Temperature of input compound into GT (°C)	1267
SOFC electrical efficiency (%)	0.4543
System electrical efficiency (%)	0.6778

Table 4. Results of simulation of hybrid system with the cathode products recycling (CRR=0.5).

Parameter	Value
Input air flow rate (kmol/s)	0.0607
Power consumed by the air compressor (kw)	239
Power output of GT (kw)	707
Power output of SOFC (kw)	1301
Net power output of system (kw)	1757
Operating temperature of SOFC (°C)	1265
Temperature of input compound into GT (°C)	1447
SOFC electrical efficiency (%)	0.5418
System electrical efficiency (%)	0.732

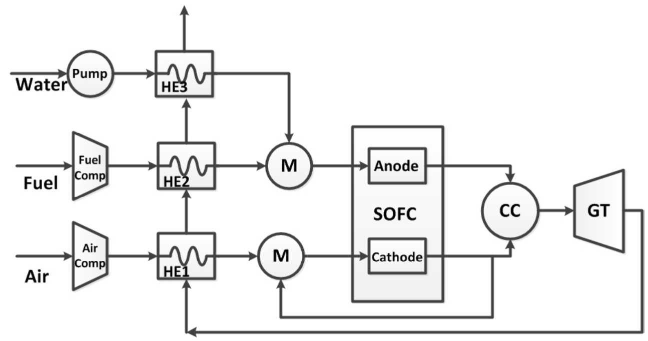

Fig. 3. Schematic of hybrid system with the cathode products recycling.

the destruction of the fuel cell and gas turbine. When CRR increases, an excessive increase of temperature can be prevented by increasing the pressure ratio or decreasing the air utilization factor. If the pressure ratio and CRR variation reache a value where the fuel cell operating temperature is equal to 1273K (at maximum value), the fuel cell and gas turbine will not be damaged. As it is seen in Fig. 4, if the pressure ratio is 2, 3, and 4, and the temperature of the fuel cell is 1273K, the CRR must be about 0.22, 0.5, and 0.63, respectively. Similarly, as it is seen in Fig.5, for the same amount of pressure ratio and CRR, the electrical efficiency is about 0.7, 0.727, and 0.745, respectively. Consequently, it was found that by increasing the pressure ratio and CRR to achieve a suitable operating temperature for the fuel cell, the total electrical efficiency of the system will increase. However, by increasing the pressure ratio, the cost of the gas turbine and compressor increased.

According to Fig. 6, if the temperature of the fuel cell equals 1273K and the air utilization factor is 0.2, 0.25, and 0.3, then the CRR must be 0.65, 0.55, and 0.4, respectively. Similarly, for the same conditions, Fig. 7 shows that the total electrical efficiency is 0.741. Consequently, the total efficiency of the system does not change by increasing the air utilization factor and decreasing the CRR.

The most suitable pressure ratio is the one leading to the maximum total efficiency of the system. This suitable pressure ratio depends on the inlet air flow rate into the system. As mentioned before, the inlet air flow rate decreases when the CRR increases. Fig. 8

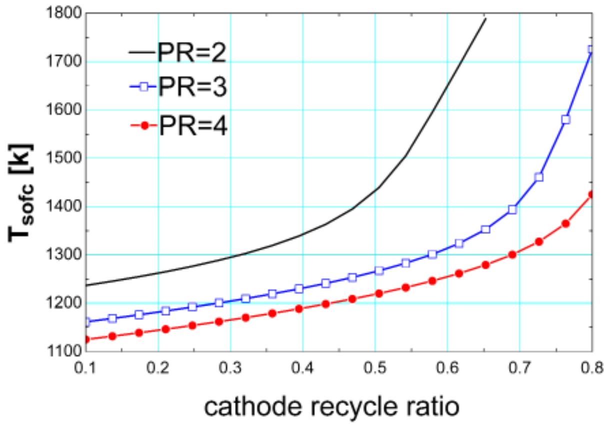

Fig. 4. Effect of the CRR on the operating temperature of fuel cell at different pressure ratio.

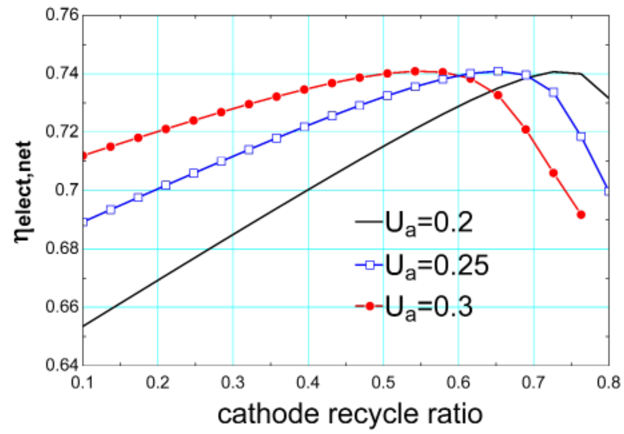

Fig. 7. Effect of the CRR on total electrical efficiency at different air utilization factor.

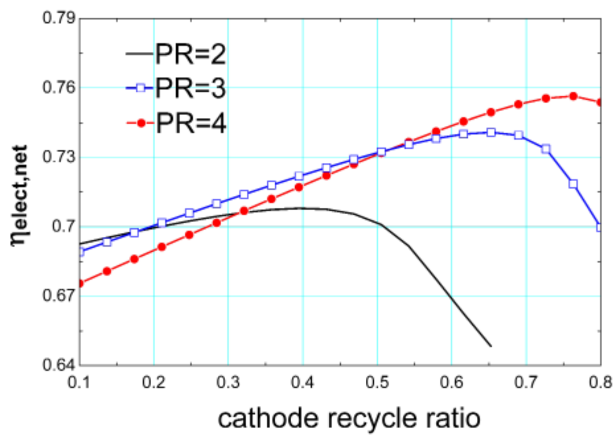

Fig. 5. Effect of the CRR on total electrical efficiency at different pressure ratio.

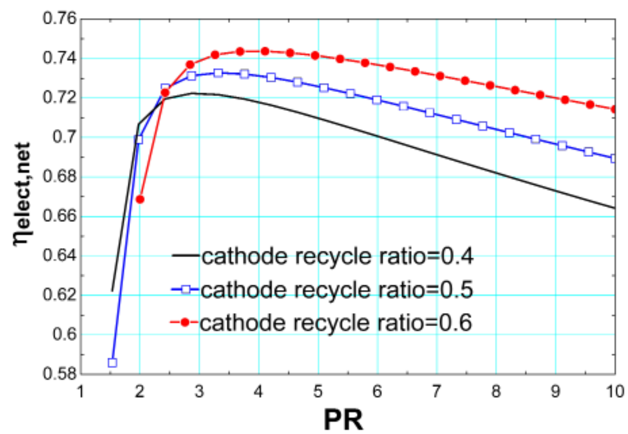

Fig. 8. Effect of pressure ratio on total electrical efficiency at different CRR.

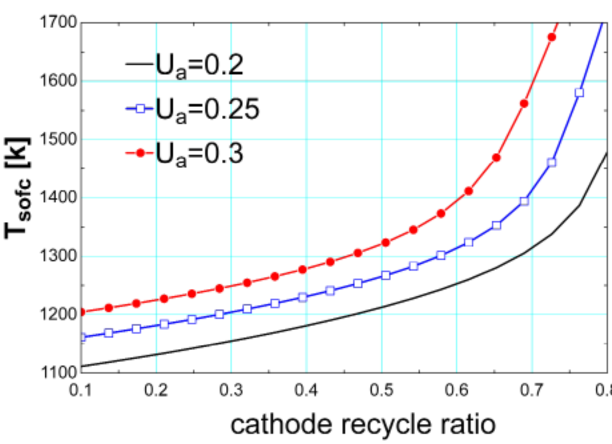

Fig. 6. Effect of the CRR on the operating temperature of fuel cell at different air utilization factor.

clearly shows that the suitable pressure ratio increases as the CRR increases.

A schematic diagram for the APR hybrid system is shown in Fig. 9. In this model, the steam required for reforming and shifting reactions is provided by anode products. A portion of the anode products that contain enough steam for reforming is combined with methane at the entrance of the anode. In addition to methane and steam, the inlet components to the anode contain carbon monoxide, carbon dioxide, and hydrogen. Because of a higher production of hydrogen, electrochemical reactions need more oxygen in this model. The results of the simulation of HS-RAP are shown in Table 5. It should be noted that the value of the anode recycle ratio (ARR) has a limitation to prevent carbon formation in the fuel cell. For this purpose, the minimum required ratio of steam to carbon is equal to 2. Fig. 10 shows that ARR should not be less than 0.55. The effect of ARR on the operating temperature of the fuel cell is shown in Figs. 11 and 12 for different pressure ratios and different air utilization factors. The ARR must choose a value where the fuel cell inlet contains the minimum required steam for chemical reactions. The operating temperature of the fuel cell increases when ARR increases, as already mentioned. Fig. 11 shows the rateof change in operating temperature decreases by increasing the ARR when the pressure ratio increases. As an example, when the ARR increases from 0.55 to 0.8 in a pressure ratio of 2, the operating temperature of the fuel cell changes from 1263 to 1306K. In a pressure ratio of 4, the operating temperature of the fuel cell changes from 1135 to 1165. new paragraph

Finally, by comparing Figs. 4 and 11, it can be seen that changes in CRR have a larger effect on the operating temperature of the fuel cell than changes in ARR. According to Fig.12, the change rate of the operating temperature of the fuel cell decreases by increasing the ARR when the air utilization factor decreases. As an example, when the air utilization factor is equal to 0.3, by increasing the ARR from 0.55 to 0.8, the operating temperature of the fuel cell changes from 1227 to 1265 K. However, for an air utilization factor of 0.2, the operating temperature of the fuel cell changes from 1117 to 1145 K. According to Fig. 13, the total efficiency of the hybrid systems slightly decreases by increasing the anode ARR. Comparison of Figs. 7 and 13 show that the effect of CRR is considerably more than ARR on electrical efficiency. The inlet air flow rate and then the optimum pressure ratio decreases when the ARR increases (Fig. 14). By comparing Figs. 8 and 14, it can seen that the effect of CRR is considerably more than ARR on the optimum pressure ratio.

In the fourth model, both anode and cathode products recycling are used as shown in Fig.15. The simulation results of this system are listed in Table 6. Comparison of BACPR-HS and CPR-HS shows that the operating temperature of the fuel cell for BACPR-HS is higher, but because of anode products recycling, the inlet temperature of the gas turbine for BACPR-HS is less. Therefore, although the BACPR-HS design is complicated, the simulation results show the advantages of this model in comparison to the other two models.

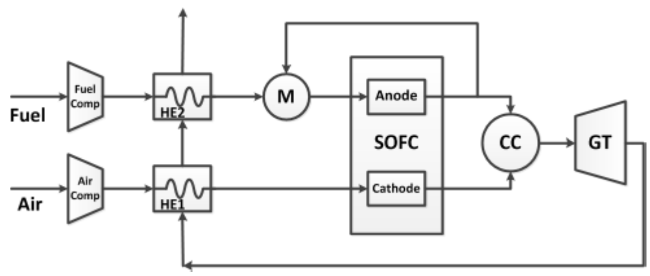

Fig. 9. Schematic of hybrid system with the anode products recycling.

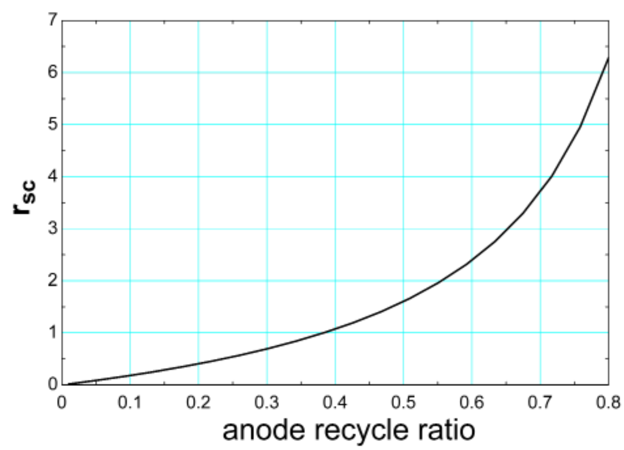

Fig. 10. Effect of the ARR on the steam to carbon ratio.

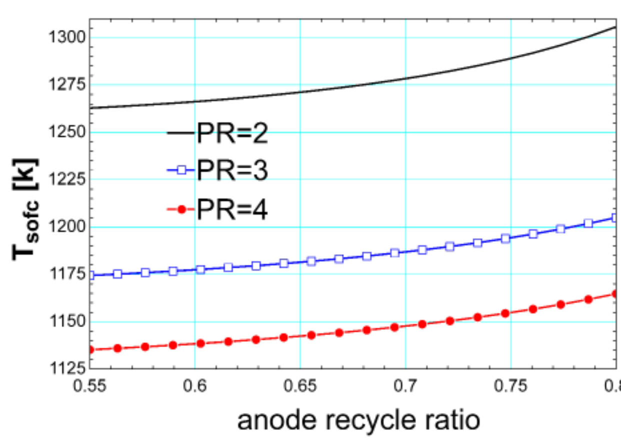

Fig. 11. Effect of ARR on the operating temperature of fuel cell at different pressure ratio.

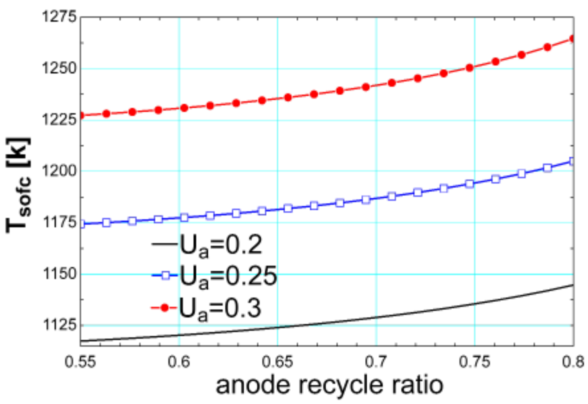

Fig. 12. Effect of the ARR on the operating temperature of fuel cell at different air utilization factor.

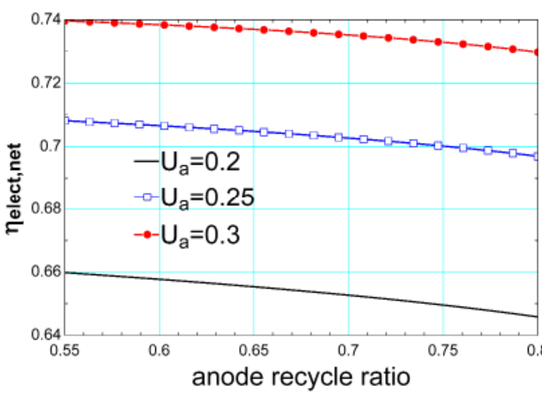

Fig. 13. Effect of the ARR on total electrical efficiency at different air utilization factor.

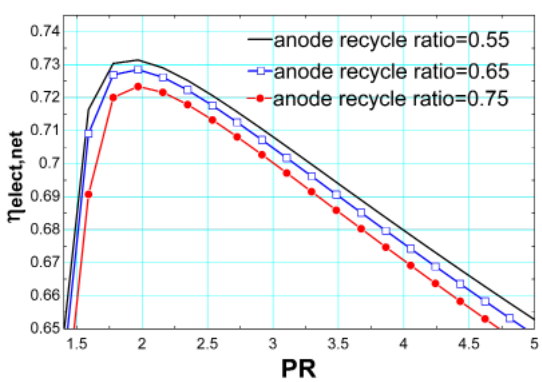

Fig. 14. Effect of pressure ratio on total electrical efficiency at different ARR.

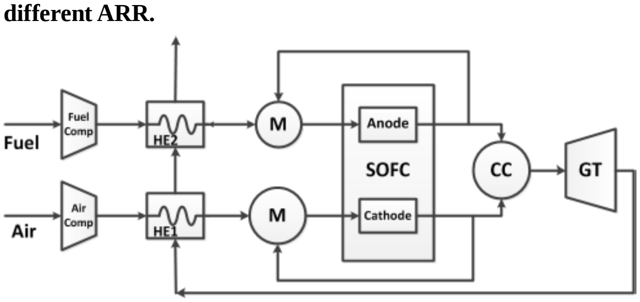

Fig. 15. Schematic of hybrid system with both cathode anode products recycling.

Table 5. Results of simulation of hybrid system with the anode products recycling ($r_{S/C}$ =2).

Parameter	Value
Input air flow rate (kmol/s)	0.106
Power consumed by the air compressor (kw)	417.2
Power output of GT (kw)	926.4
Power output of SOFC (kw)	1202
Net power output of system (kw)	1700
Operating temperature of SOFC (°C)	1175
Temperature of input compound into GT (°C)	1236
SOFC electrical efficiency (%)	0.5006
System electrical efficiency (%)	0.708

Table 6. Results of simulation of Hybrid system with both cathode and anode products recycling (CRR=0.35, $r_{S/C}$ =2).

Parameter	Value
Input air flow rate (kmol/s)	0.07819
Power consumed by the air compressor (kw)	307.8
Power output of GT (kw)	759.8
Power output of SOFC (kw)	1372
Net power output of system (kw)	1813
Operating temperature of SOFC (°C)	1271
Temperature of input compound into GT (°C)	1351
SOFC electrical efficiency (%)	0.5717
System electrical efficiency (%)	0.7553

6. Conclusions

In this study, the effect of solid oxide fuel cell products recycling on the performance of SOFC-GT hybrid system was investigated. The hybrid system includes three types of products recycling: cathode products recycling, anode products recycling, and both cathode and anode products recycling.

The following main results were obtained:

- Fuel cell products recycling improves the net power output and the total efficiency of the hybrid system.
- The operating temperature of the fuel cell increases as CRR increases. Therefore, the net output power and the efficiency of the fuel cell increase.
- By increasing CRR to improve the performance of the fuel cell at a desired operating temperature, the pressure ratio must be set at a higher value.
- When the CRR increases to achieve a desired

operating temperature, the air utilization factor decreases to a lower value.

- Two conditions must be satisfied to choose the correct CRR. First, the selected operating temperature of the fuel cell and the gas turbine should be less than the permissible temperature. Second, the amount of required oxygen in the combustion chamber should be enough to complete combustion.

- The ARR value must be chosen so that the minimum required steam becomes available for reactions in the SOFC.

. A steam shortage causes a carbon deposition on the anode electrode and excessive voltage losses.

- CRR is more effective in improving the net output power and total efficiency of the hybrid system in comparison with ARR.

- The hybrid system with both cathode and anode products recycling has advantages in comparison with the two others systems, these include higher total electrical efficiency and a lower inlet temperature into the gas turbine.

Nomenclature

D_{eff}	effective gas diffusion factor (m^2/s)
E	reversible voltage of the fuel cell (V)
E^0	fuel cell voltage under standard conditions (V)
E_{act}	activation energy (kJ/kmol)
F	Faraday's constant (96,485 C/mol)
h	enthalpy (kJ/kmol)
i	current density (A/ m^2)
i_0	exchange current density (A/ m^2)
i_L	limiting current density (A/ m^2)
I	current (A)
K_p	equilibrium constant
LHV	low heating value (kJ/kmol)
M	molecular weight (kg/kmol)
n	molar flow rate (kmol/s)
n_e	number of electron
P	pressure (kPa)
PR	compression ratio
Q	heat generation rate (kW)
r	ohmic resistance (Ω)
r_{por}	average pore radius
$r_{S/C}$	ratio of steam to carbon
R_u	universal gas constant (8.314 J/mol K)
s	entropy (kJ/kmol K)
T	temperature (K)
U_a	air utilization coefficient
U_f	fuel utilization coefficient
V_{act}	activation loss (V)
V_{cell}	cell voltage (V)
V_{conc}	concentration loss (V)
V_{loss}	voltage loss (V)
V_{ohm}	ohmic loss (V)
W	electrical power (kW)
x	molar rates of progress of the cell reforming reactions (kmol/s)
y	molar rates of progress of the cell shifting reactions (kmol/s)
z	molar rates of progress of the cell electrochemical reactions (kmol/s)

Greek letters

ε	porosity
η	efficiency
ρ	resistivity (Ω m)
τ	tortuosity
υ	special Fuller diffusion volume
ε_{He}	efficiency of heat exchanger

Subscripts

a	air
an	anode
ca	cathode
cc	combustion chamber
cell	fuel cell
comp	compressor
elec	electrochemical reactions
elect	electrical
f	fuel
g	gas
gt	gas turbine
He	heat exchanger
in	inlet

invt	inverter
is	isentropic
out	exit
r	reforming reaction
sh	shifting reaction
surr	surrounding

Acronyms

SOFC	solid oxide fuel cell
GT	gas turbine
S-HS	Standard hybrid system
HS-RCP	hybrid system with the recycle of cathode products
HS-RAP	hybrid system with the recycle of anode products
HS-RCAP	hybrid system with the recycle of cathode and anode products
CRR	cathode recycle ratio
ARR	anode recycle ratio

References

[1] Reijalt M. Hydrogen and fuel cell education in Europe: from when? And where? To here! And now!.Journal of Cleaner Production,18, pp.112-117, 2010.

[2] Williams MC. Fuel cell handbook.EG&G Technical Services, Inc, West Virginia, 2004.

[3] Singhal SC. Advances in Solid Oxide Fuel Cells.Journal of Solid State Ionic, 135, pp.305-313, 2000.

[4] Chan SH, Khor KA, Xia ZT.A complete polarization model of a solid oxide fuel cell and its sensitivity to the change of cell component thickness.Journal of Power Sources,93, pp.130-140, 2001.

[5] Chan SH, Ho HK, TianY.Modeling of simple hybrid solid oxide fuel cell and gas turbine power plant.Journal of Power Sources ,109,pp. 111-120, 2002.

[6] Volkan Akkaya A. Electrochemical Model for Performance Analysis of a Tubular SOFC.International Journal ofEnergy Research, 31, pp.79-98, 2007.

[7] GhanbariBavarsad P. Energy and exergy analysis of internal reforming solid oxide fuelcellegas turbine hybrid system. International Journal of Hydrogen Energy 32,pp. 4591-4599, 2007.

[8] Pirkandi J, Ghassemi M, Hamedi MH, Mohammadi R. Electrochemical and thermodynamic modeling of a CHP system using tubular solid oxide fuel cell (SOFC-CHP). Journal of Cleaner Production, 29,30,pp. 151-162, 2012.

[9] Aloui T, Halouani K. Analytical modeling of polarizations in a solid oxide fuel cell using biomass syngas product as fuel.Applied Thermal Engineering, 27 ,pp. 731–737, 2007.

[10] Haseli Y, Dincer I, Naterer GF. Thermodynamic Modeling of a Gas Turbine Cycle Combined with a Solid Oxide Fuel Cell.InternationalJournal of Hydrogen energy, 33, pp. 5811-5822, 2008.

[11] Motahar S,Alamrajabi AA, Exergy Based Performance Analysis of a Solid Oxide Fuel Cell and Steam Injected Gas Turbine Hybrid Power System.International journal of hydrogen energy, 34, pp. 2396-2407, 2009.

[12] Calise F, Palombo A, VanoliL. Design and partial load exergy analysis of hybrid SOFC–GT power plant. Journal of Power Sources, 158,pp. 225–244, 2006.